Article

Medicinal Chemistry Friendliness of Pigments from Monascus-Fermented Rice and the Molecular Docking Analysis of Their Anti-Hyperlipidemia Properties

Nina Sun [1] , Dominic Agyei [2] and Dawei Ji [2],*

[1]   CapitalBio Technology, Beijing 101111, China; ninasun1205@163.com
[2]   Department of Food Science, University of Otago, Dunedin 9054, New Zealand; dominic.agyei@otago.ac.nz
*   Correspondence: jidawei2008@gmail.com; Tel.: +64-21-1642461

check for updates

Abstract: In this study, the physicochemical properties, pharmacokinetics properties, and drug-likeness of pigments from *Monascus*-fermented rice (*Monascus* pigments, MPs) were predicted in silico using SwissADME tool. In silico prediction of physicochemical properties showed that MPs had desirable lipophilic drug-like physicochemical properties including molecular weight (236 to 543), TPSA (44.76 to 179.77), lipophilicity (−0.81 to 4.14), and water solubility (−4.94 to −0.77). The pharmacokinetic properties of MPs (i.e., GIA, P-glycoprotein substrate, and CYP3A4 inhibitor) illustrated that most MPs had high intestinal absorption and bioavailability, but some MPs might cause pharmacokinetics-related drug–drug interactions. Following this, six main well-known MPs (monascin, ankaflavin, rubropunctatin, monascorubrin, rubropunctamine, monascorubramine) were selected for molecular docking with some enzyme receptors. The docking results were shown with the best molecular docking poses, and the interacting residues, number and distance of hydrogen bonds of the MPs and monacolin K (for docking with 3-hydroxy-3-methyl glutaryl coenzyme A reductase (HMG-CoA reductase)), or MPs and oleic acid (for docking with lipase). Dissociation constants showed that MPs had lower inhibitory potential for HMGR (compared with Monacolin K), and higher inhibitory potential for lipase. Individual pigments from *Monascus*-fermented rice, therefore, have the potential to be developed as drug candidates for controlling hyperlipidemia.

Keywords: *Monascus* pigments; hyperlipidemia; HMG-CoA reductase; lipase; in silico evaluation; molecular docking

1. Introduction

Hyperlipidemia refers to acquired or genetic disorders resulting in high levels of cholesterol, triglycerides (TG), free fatty acids, and low-density lipoprotein cholesterol (LDL-C) in the blood circulation, along with an excessive accumulation of TG in the liver [1]. Hyperlipidemia has become a global public health problem as a risk factor for strokes or heart attacks [2,3]. Individuals with hyperlipidemia have responded well to lipid-lowering agents such as statins, nicotinic acids, and fibrates [4]. However, nowadays, many people prefer to use nutraceuticals due to interest in 'natural' avenues of disease control, and the concern of potential drug interactions, long-term safety, and the economic implications of long-term (or life-long) dependence on drugs [5,6]. Moreover, some of the medications used to treat hyperlipidemia e.g., statins have side effects such as nausea, headaches, myalgias, memory loss and cognitive function impairment, and increased risk of diabetes [7–11].

Monascus fermented rice has been used as a functional food worldwide for decades [12,13]. A large number of studies has shown that *Monascus* fermented rice is effective in hyperlipidemia

treatment [2,14,15]. Monacolin K (also called lovastatin), one of the statin medications, is widely considered to be the most efficacious compound in *Monascus* fermented rice to treat high blood cholesterol by inhibiting 3-hydroxy-3-methyl glutaryl coenzyme A reductase (HMG-CoA reductase or HMGR), the rate-limiting enzyme in cholesterol biosynthesis [13]. However, the proportion of Monacolin K in *Monascus* products is relatively low, suggesting there might be other compounds having antihyperlipidemic effects [16–18].

Besides Monacolin K, *Monascus* pigments (MPs) have shown antihyperlipidemic effects in several previous studies. For example, Zhou, et al. [19] reported that *Monascus* yellow, red, and orange pigments can significantly decrease the levels of serum lipid (cholesterol, TG, free fatty acids and LDL-C), and suppressed hepatic lipid accumulation in Wistar rats fed on a high-fat diet. In addition, Fang, et al. [20] pointed out that 3 pigments from *Monascus* fermented rice, monascin, monasfluore B, and ankaflavin, can be used as inhibitors of pancreatic lipase, another critical enzyme associating with hyperlipidemia. However, the mechanism of *Monascus* pigments in treating hyperlipidemia has not been intensively studied.

A number of studies have reported a wide range of health beneficial pigment compounds present in MPs [21–24]. The production of toxic secondary metabolites (e.g., citrinin, a nephrotoxic mycotoxin) by *Monascus* species has also been reported [25–27]. However, a review of the literature shows that, in most research on this topic, extracted pigment mixtures rather than individual compounds, are used. This makes it challenging to ascribe a desired property to a particular compound. Moreover, although the chemical identities of several *Monascus* secondary metabolites have been unraveled [24,28], the potential health properties of most of these compounds (in pure preparations) are unknown. Based on their health application prospects, it is necessary to unravel the potential bioactive properties (both drug-likeness and toxicity) of these compounds. The challenge though is that there is a huge list to work with. For example, the chemical structures of a total of 61 of MPs have been reported by Yuliana, et al. [22], and Feng, et al. [24]. Using conventional methods to characterize the biological properties of such a large number of MPs is time-consuming, labor-intensive, and costly. However, in silico and bioinformatics tools have been shown to be useful in studying the potential drug-likeness of biomolecules quickly and in a cost-effective manner [29–32]. Therefore, in this work, in silico tools were used to predict and evaluate the physicochemical and pharmacokinetic properties of 61 MPs, and evaluate their in silico drug-likeness. The molecular docking interactions of six well-known MPs (monascin, ankaflavin, rubropunctatin, monascorubrin, rubropunctamine, monascorubramine) with both HMG-CoA reductase and lipase were studied. The binding energies and computational dissociation constants of the six MPs were also compared with those of monacolin K (for HMG-CoA reductase) and oleic acid (for lipase) to ascertain the anti-hyperlipidemia properties of the six MPs.

2. Methods

2.1. Preparation of Monascus Pigments (Docking Ligand)

The molecular structures of *Monascus* pigments were prepared according to a previous review by Yuliana, et al. [22] and Feng, et al. [24], or by being downloaded from PubChem (https://pubchem.ncbi.nlm.nih.gov/). Sixty-one (61) MPs were used, representative of 26 yellow pigments, 6 orange pigments, and 29 red pigments. Six well-known MPs produced by *Monascus* were selected for docking experiments, including monascine (yellow), angkakflavin (yellow), rubropunctatin (orange), monascorubrine (orange) and (red) rubropuntantamine (red), monascorubramine (red). The structural and empirical formulae of the 61 MPs is shown in Table 1.

Table 1. Chemical structures of the 61 *Monascus* pigments (MPs) used in this study.

No.	Color	Name	Canonical SMILES	Molecular Formula
1	yellow	monascin	CCCCCC(=O)C1C(=O)OC2(C1CC1=C(C2=O)COC(=C1)/C=C/C)C	$C_{21}H_{26}O_5$
2	yellow	ankaflavin	CCCCCCCC(=O)C1C(=O)OC2(C1CC1=C(C2=O)COC(=C1)/C=C/C)C	$C_{23}H_{30}O_5$
3	orange	rubropunctatin	CCCCCC(=O)C1=C2C=C3C=C(/C=C/C)OC=C3C(=O)C2(OC1=O)C	$C_{21}H_{22}O_5$
4	orange	monascorubrin	CCCCCCCC(=O)C1=C2C=C3C=C(/C=C\C)OC=C3C(=O)C2(OC1=O)C	$C_{23}H_{26}O_5$
5	red	rubropunctamine	CCCCCC(=O)C1=C2C=C3C=C(NC=C3C(=O)C2(C)OC1=O)\C=C\C	$C_{21}H_{23}NO_4$
6	red	monascorubramine	CCCCCCCC(=O)C1=C2C=C3C=C(NC=C3C(=O)C2(C)OC1=O)\C=C\C	$C_{23}H_{27}NO_4$
7	yellow	xanthomonasin A	CCCCCC(=O)C1=C2c3oc(c(c3C[C@@]([C@]2(OC1=O)C)(O)/C=C/C)C=O)O	$C_{21}H_{24}O_7$
8	yellow	xanthomonasin B	CCCCCCCC(=O)C1=C(O)O[C@]2(C1=C1OC(=O)C(=C1C[C@@]2(O)/C=C/C)C=O)C	$C_{23}H_{28}O_7$
9	yellow	yellow II	CCCCCCCC(=O)C1=C(O)OC2(C1=CC1=C/C(=C/C)/OCC1C2=O)C	$C_{22}H_{28}O_5$
10	yellow	monankarin A	C[C@@H]1CC(=O)C=C(O1)c1cc2c(oc1=O)cc(c(c2[C@@H]([C@H](O)C)C)C)O	$C_{20}H_{22}O_6$
11	yellow	monankarin B	C[C@@H]1CC(=O)C=C(O1)c1cc2c(oc1=O)cc(c(c2[C@@H]([C@H](O)C)C)C)O	$C_{20}H_{22}O_6$
12	yellow	monankarin C	CC1CC(=O)C=C(O1)c1cc2c([C@H]([C@H](O)C)C)c(c(c2oc1=O)C)O	$C_{21}H_{24}O_6$
13	yellow	monankarin D	CC1CC(=O)C=C(O1)c1cc2c([C@@H]([C@@H](O)C)C)c(C)c(c(c2oc1=O)C)O	$C_{21}H_{24}O_6$
14	yellow	monankarin E	CC(Cc1cc(O)c(c2c1cc(C1=CC(=O)CC(O1)C)c(=O)o2)C)O	$C_{19}H_{20}O_6$
15	yellow	monankarin F	CC1CC(=O)C=C(O1)c1cc2c(CC(O)C)c(C)c(c(c2oc1=O)C)O	$C_{20}H_{22}O_6$
16	yellow	monascusone A	C[C@@H](CC1=CC2=C(CO1)C(=O)[C@]([C@H](C2)O)(C)O)O	$C_{13}H_{18}O_5$
17	yellow	monascusone B	C/C=C/C1=CC2=C(CO1)C(=O)[C@]1([C@H](C2)[C@@H](C(=O)C)C(=O)O1)C	$C_{17}H_{18}O_5$
18	yellow	FK17-P2B2	C/C=C/C1=CC2=C(CO1)C(=O)[C@]([C@H](C2)O)(C)O	$C_{13}H_{16}O_4$
19	yellow	Y3	CC(CC(C(CC(=O)O)(O)C)(c1c(OC(=S)CC(O)C)cc(c(c1O)C)O)O)C	$C_{20}H_{30}O_8S$
20	yellow	monaphilone A	CCCCCCCC(=O)C[C@H]1CC2=C(C(=O)[C@]1(C)O)COC(=C2)/C=C/C	$C_{22}H_{32}O_4$
21	yellow	monaphilone B	CCCCCC(=O)C[C@H]1CC2=C(C(=O)[C@]1(C)O)COC(=C2)/C=C/C	$C_{20}H_{28}O_4$
22	yellow	monaphilone C	CCCCCC(=O)C[C@@H]1CC(=C(C(=O)[C@]1(C)O)C)CC(=O)CCC	$C_{20}H_{32}O_4$
23	yellow	monapurone A	CCCCCC(=O)C[C@@H]1C2=COC(=CC2=CC(=O)[C@]1(C)O)/C=C/C	$C_{20}H_{26}O_4$
24	yellow	monapurone B	CCCCC[C@@]1(OC)C[C@H]2[C@](O1)(C)C(=O)C=C1C2=COC(=C1)/C=C/C	$C_{21}H_{28}O_4$
25	yellow	monapurone C	CCCCC[C@]1(OC)C[C@H]2[C@](O1)(C)C(=O)C=C1C2=COC(=C1)/C=C/C	$C_{21}H_{28}O_4$
26	yellow	monarubrin	CCCCCC(=O)CC1C=C2C=C(/C=C/C)OC=C2C(=O)C1(C)O	$C_{20}H_{26}O_4$
27	yellow	rubropunctin	CCCCCCCC(=O)CC1C=C2C=C(/C=C/C)OC=C2C(=O)C1(C)O	$C_{22}H_{30}O_4$
28	orange	monapilol A	CCCCCCCC(=O)C1=C2C=C3C=C(/C=C/C)OC=C3[C@@H]([C@@]2(OC1=O)C)O	$C_{23}H_{28}O_5$
29	orange	monapilol B	CCCCCC(=O)C1=C2C=C3C=C(/C=C/C)OC=C3[C@@H]([C@@]2(OC1=O)C)O	$C_{21}H_{24}O_5$
30	orange	monapilol C	CCCCCCCC(=O)C1=C2C=C3C=C(/C=C/C)OC=C3[C@]([C@@]2(OC1=O)C)(O)CC(=O)C	$C_{26}H_{32}O_6$

Table 1. *Cont.*

No.	Color	Name	Canonical SMILES	Molecular Formula
31	orange	monapilol D	CCCCCC(=O)C1=C2C=C3C=C(/C=C/C)OC=C3[C@]([C@@]2(OC1=O)C)(O)CC(=O)C	$C_{24}H_{28}O_6$
32	red	N-glucosylrubropunctamine	CCCCCC(=O)C1=C2C=c3cc(/C=C/C)n(cc3C(=O)[C@@]2(OC1=O)C)[C@H]1OC(CO)[C@@H]([C@H](C1O)O)O	$C_{30}H_{37}NO_{11}$
33	red	N-glucosylmonascorubramine	CCCCCCCC(=O)C1=C2C=c3cc(/C=C/C)n(cc3C(=O)[C@@]2(OC1=O)C)[C@H]1OC(CO)[C@@H]([C@H](C1O)O)O	$C_{32}H_{41}NO_{11}$
34	red	N-glutarylrubropunctamine	CCCCCC(=O)C1=C2C=c3cc(/C=C/C)n(cc3C(=O)C2(OC1=O)C)C(C(=O)O)CCC(=O)O	$C_{26}H_{29}NO_8$
35	red	N-glutarylmonascorubramine	CCCCCCCC(=O)C1=C2C=c3cc(/C=C/C)n(cc3C(=O)C2(OC1=O)C)C(C(=O)O)CCC(=O)O	$C_{28}H_{33}NO_8$
36	red	Red Derivat 1	CCCCCCCC(=O)C1=C2C=c3cc(/C=C/C)n(cc3C(=O)[C@@]2(OC1=O)C)[C@H](C(=O)O)C	$C_{26}H_{31}NO_6$
37	red	Red Derivat 2	CCCCCC(=O)C1=C2C=c3cc(/C=C/C)n(cc3C(=O)[C@@]2(OC1=O)C)[C@H](C(=O)O)C	$C_{24}H_{27}NO_6$
38	red	Red Derivat 3	CCCCCCCC(=O)C1=C2C=c3cc(/C=C/C)n(cc3C(=O)[C@@]2(OC1=O)C)[C@H](C(=O)O)CC(=O)O	$C_{27}H_{31}NO_8$
39	red	Red Derivat 4	CCCCCC(=O)C1=C2C=c3cc(/C=C/C)n(cc3C(=O)[C@@]2(OC1=O)C)[C@H](C(=O)O)CC(=O)O	$C_{25}H_{27}NO_8$
40	red	Red Derivat 5	CCCCCCCC(=O)C1=C2C=c3cc(/C=C/C)n(cc3C(=O)[C@@]2(OC1=O)C)[C@@H](C(=O)O)C	$C_{26}H_{31}NO_6$
41	red	Red Derivat 6	CCCCCC(=O)C1=C2C=c3cc(/C=C/C)n(cc3C(=O)[C@@]2(OC1=O)C)[C@@H](C(=O)O)C	$C_{24}H_{27}NO_6$
42	red	Red Derivat 7	CCCCCCCC(=O)C1=C2C=c3cc(/C=C/C)n(cc3C(=O)[C@@]2(OC1=O)C)[C@@H](C(=O)O)CC(=O)O	$C_{27}H_{31}NO_8$
43	red	Red Derivat 8	CCCCCC(=O)C1=C2C=c3cc(/C=C/C)n(cc3C(=O)[C@@]2(OC1=O)C)[C@@H](C(=O)O)CC(=O)O	$C_{25}H_{27}NO_8$
44	red	R3	CCCCCC(=O)C1C(=O)OC2(C1C1=COC(=CC1=CC2=O)CC(O)C)C	$C_{21}H_{26}O_6$
45	red	Unamed	C/C=C/C1=CC2=CC3=[O+]NOC3C(C2CN1C(C(=O)O)CCCCN)O)C	$C_{19}H_{28}N_3O_5$
46	red	PP-V	CCCCCCCC(=O)C1=C2C=C3C=C(/C=C\C(=O)[O-])[NH2+]C=C3C(=O)C2(OC1=O)C	$C_{23}H_{25}NO_6$
47	red	New Red Pigment	CCCCCC(C1C(=O)OC2(C1c1c[nH]c(cc1=CC2=O)CC(O)C)C)O	$C_{21}H_{29}NO_5$
48	red	Isolate MPs 1	CCCCCC(=O)C1=C2C=c3cc(/C=C/C)n(cc3C(=O)C2(OC1=O)C)C(C(=O)O)CCCNC(=N)N	$C_{27}H_{34}N_4O_6$
49	red	Isolate MPs 2	CCCCCCCC(=O)C1=C2C=c3cc(/C=C/C)n(cc3C(=O)C2(OC1=O)C)C(C(=O)O)CCCNC(=N)N	$C_{29}H_{38}N_4O_6$
50	red	Isolate MPs 3	CCCCCCCC(=O)C1=C2C=c3cc(/C=C/C)n(cc3C(=O)C2(OC1=O)C)CC(=O)O	$C_{25}H_{29}NO_6$
51	red	glycyl-rubropunctatin	CCCCCC(=O)C1=C2CC3=C(C(=O)[C@@]2(OC1=O)C)CN(C(=C3)/C=C/C)CC(=O)O	$C_{23}H_{27}NO_6$
52	red	Isolate MPs 4	CCCCCCCC(=O)C1=C2CC3=C(C(=O)[C@@]2(OC1=O)C)CN(C(=C3)/C=C/C)CC(=O)O	$C_{25}H_{31}NO_6$
53	red	Monascopyridine A	CCCCCC(=O)[C@@H]1C(=O)O[C@]2([C@H]1Cc1cc(/C=C/C)ncc1C2=O)C	$C_{21}H_{25}NO_4$
54	red	Monascopyridine B	CCCCCCCC(=O)[C@@H]1C(=O)O[C@]2([C@H]1Cc1cc(/C=C/C)ncc1C2=O)C	$C_{23}H_{29}NO_4$
55	red	Monascopyridine C	CCCCCC(=O)C[C@@H]1Cc2cc(/C=C/C)ncc2C(=O)[C@@]1(C)O	$C_{20}H_{27}NO_3$
56	red	Monascopyridine D	CCCCCCCC(=O)C[C@@H]1Cc2cc(/C=C/C)ncc2C(=O)[C@@]1(C)O	$C_{22}H_{31}NO_3$
57	yellow	Monasfluore A	CCCCCC(=O)C1C(=O)OC2(C1C1=COC(=CC1=CC2=O)/C=C/C)C	$C_{21}H_{24}O_5$
58	yellow	Monasfluore B	CCCCCCCC(=O)C1C(=O)OC2(C1C1=COC(=CC1=CC2=O)/C=C/C)C	$C_{23}H_{28}O_5$
59	yellow	purpureusone	CCCCCCCC(=O)[C@H]1C(=O)O[C@@]2(C1CC(=C(C2=O)C)CC(=O)CCC)C	$C_{23}H_{34}O_5$
60	red	Red Shandong 1	C=CCCCC(C1=CC2=C/C(=C/C=C)/NCC2C(C1O)O)O	$C_{18}H_{25}NO_3$
61	red	Red Shandong 2	C=CCCCCCC(C1=CC2=C/C(=C/C=C)/NCC2C(C1O)O)O	$C_{20}H_{29}NO_3$

2.2. In Silico Evaluation of Physicochemical Properties and Drug-Likeness of Monascus Pigments

In silico evaluation of physicochemical properties and drug-likeness for the 61 *Monascus* pigments was evaluated using the SwissADME tool (http://www.swissadme.ch/index.php#). This tool computes physicochemical properties (molecular weight, TPSA (topological polar surface area), lipophilicity, and water solubility), and estimates the indicators of pharmacokinetics (GIA (gastrointestinal absorption), P-glycoprotein (permeability glycoprotein or multidrug resistance protein 1) substrate, and CYP3A4 inhibitor (cytochrome P450 3A4 inhibitor)) as well as drug-likeness and bioavailability of MPs.

2.3. Molecular Docking

Molecular docking was performed using the Discovery Studio software 2019 (DS 2019) and Autodock Vina. For docking onto HMG-CoA Reductase receptor, a crystal structure of human HMG-CoA Reductase (1HW9 (PDB) bound with simvastatin (an HMG-CoA Reductase inhibitor) was used. The simvastatin and water molecules were removed, and polar hydrogen atoms were added prior to docking. A binding site was searched in a box of $24 \times 24 \times 24$ Å with centered on the coordinates x: 10.8, y: 10.8 and z: 13.6. For lipase docking, a crystal structure of porcine lipase 1ETH (PDB) was used. Unnecessary structures such as water molecules and metals were removed, and polar hydrogen atoms were added. A binding site was searched in a box of $24 \times 24 \times 24$ Å with centered on the coordinates x: 63.7, y: 28.5, z: 120.6, and automated molecular docking was then performed using Autodock Vina. In the docking process, the ligand was flexible, while the receptor (protein) was rigid. All generated docking modes were evaluated according to affinity energy values. The dissociation constant (K_i) were calculated using affinity energy according to our previous study [33]. The DS 2019 software was utilized to view hydrogen bonds as well as hydrophilic, hydrophobic, and electrostatic interactions between residues at the HMG-CoA Reductase or lipase active sites and the pigment compounds.

3. Results and Discussion

3.1. Physicochemical Properties of Monascus Pigments

The physicochemical characteristics of MPs are presented in Figure 1. The mol. wt. of 61 MPs ranged from 236 to 543. Twenty-six (26) yellow MPs and 6 orange MPs had a mol. wt. range of 236–430 and 354–440, respectively, while 29 red MPs had mol. Wt. between 353 and 543 (Figure 1A). The mol. wt. of most (56) MPs were less than 500 in accordance with the rules-of-five [34]. Only 5 red MPs had mol. wt. greater than 500.

Topological polar surface area (TPSA) is a critical descriptor in many estimation models and rules of drug-likeness or bioavailability, especially in regards to absorption [35]. TPSA ranges of 20–130 Å^2 are indicative of the compound having the ability to permeate into cells [36]. The TPSA of MPs were in the range of 44.76 to 179.77. As shown in Figure 1B, 25 yellow MPs and 19 red MPs and all 6 orange MPs were in the acceptable TPSA ranges (20–130 Å^2), while one yellow MPs and 10 red MPs had lager TPSA (>130 Å^2). The results suggested yellow MPs and orange MPs would have better bioavailability and absorption into cells than red MPs.

The lipophilicity of MPs was calculated by using the partition coefficient between n-octanol and water (log $P_{o/w}$) [37]. To increase the prediction accuracy, consensus Log $P_{o/w}$ was conducted, which is the average of five predictive methods (iLOGP, XLOGP3, WLOGP, MLOGP and SILICOS-IT) [37]. The lipophilicity of MPs ranged from −0.81 to 4.14. The yellow MPs had a lipophilicity range of 0.4 to 4.14, red MPs ranged from −0.81 to 4.09, while orange MPs ranged between 2.98 and 4.04 (Figure 1C). The lipophilicity of all MPs was below 5, implying they have good permeability across the cell membrane, while only two MPs (one red and one yellow) had lipophilicity below 1. This shows that most MPs are more lipophilic and less water-soluble [34].
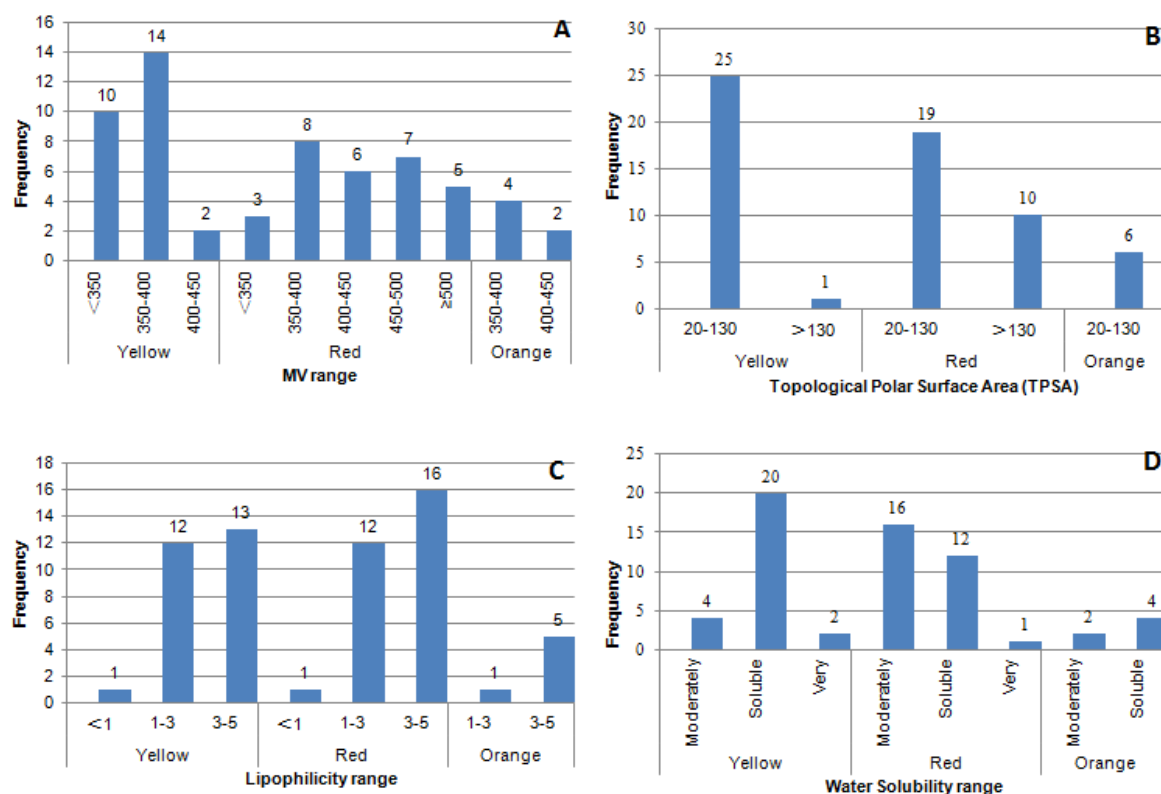
Figure 1. Distribution of physicochemical properties (**A**). molecular weight; (**B**). Topological polar surface area (TPSA); (**C**). Lipophilicity; (**D**). Water Solubility) of the *Monascus* pigments.

The water solubility is also an important parameter, since a high Log *S* values correspond to good drug absorption [38]. The Log *S* of MPs were calculated with method ESOL, and a qualitative estimation of the solubility class is given according to the following scale: Insoluble < −10 < Poorly soluble < −6 < Moderately soluble < −4 < Soluble <−2 < Very soluble < 0 < Highly soluble [39]. The water solubility of MPs ranged from −4.94 to −0.77. Yellow MPs had a water solubility range of −4.40 to −0.77, in which only 3 are Moderately soluble, and 23 are Soluble and/or Very soluble. In contract, red MPs had a water solubility range of −4.94 to −0.86, in which 16 are Moderately soluble, and 13 are Soluble and/or Very soluble. Orange MPs ranged from −4.4 to −3.06, in which 2 are Moderately soluble, and 4 are Soluble (Figure 1D). Therefore, the water solubility results suggested yellow MPs would have better drug absorption compared with red MPs.

3.2. Pharmacokinetics Properties

The pharmacokinetics and drug-likeness of all the 61 *Monascus* pigments were predicted using physicochemical and ADME properties calculated from SwissADME [37]. As shown in Figure 2, the pharmacokinetics were evaluated by GIA (gastrointestinal absorption), P-glycoprotein (permeability glycoprotein or multidrug resistance protein 1) substrate, and CYP3A4 inhibitor (cytochrome P450 3A4 inhibitor).

The prediction of GIA is based on the Brain Or IntestinaL EstimateD permeation (BOILED Egg) model, which uses lipophilicity and polarity of molecules to predict passive gastrointestinal absorption of compounds [35]. The Predicted GIA of 50 MPs (including 25 yellow MPs and 6 orange MPs and 19 red MPs) were high, while one yellow MP and 10 red MPs had low GIA (Figure 2A). That indicated yellow MPs and orange MPs could have better passive gastrointestinal absorption compared with red MPs.
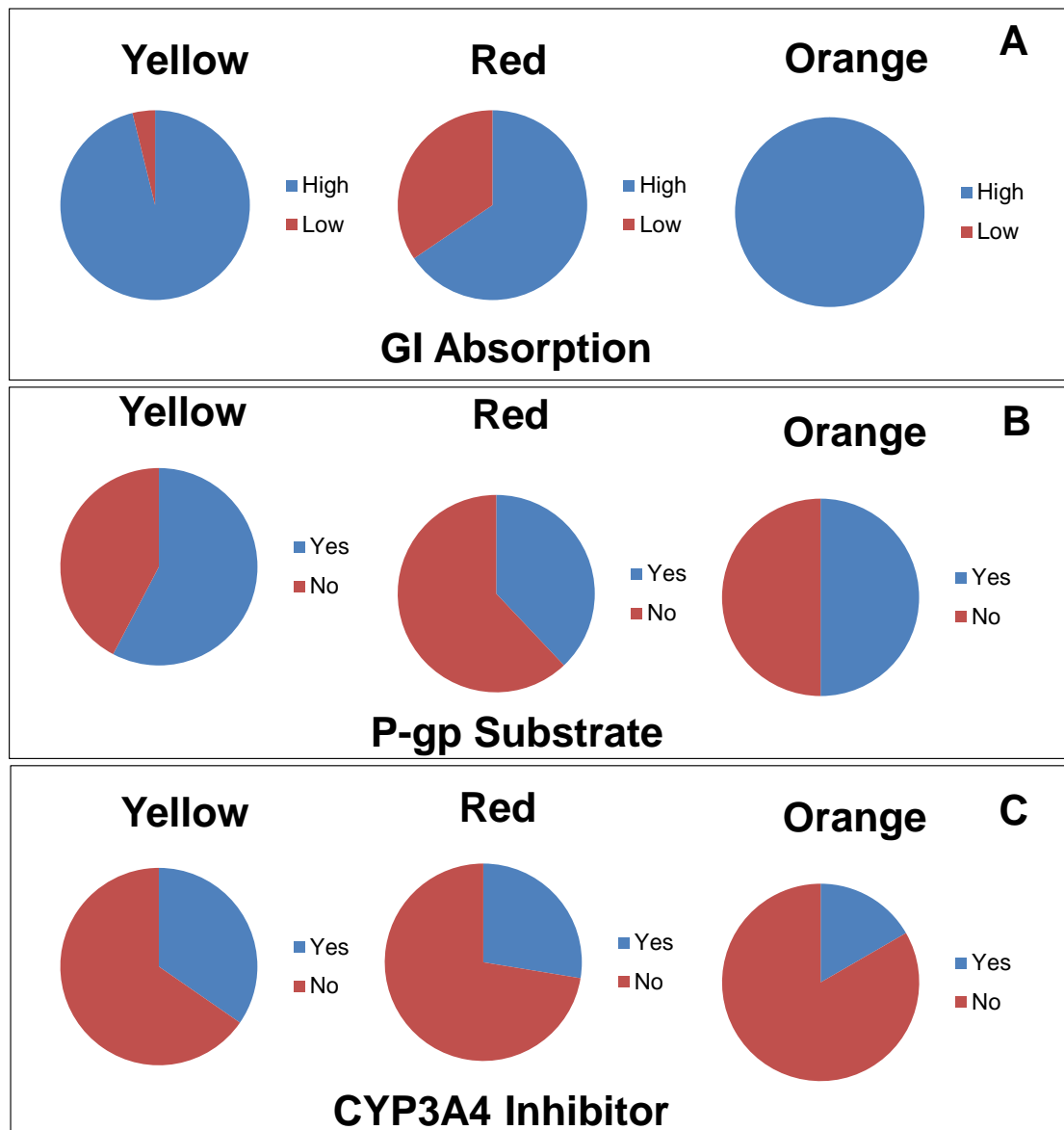
Figure 2. Distribution of pharmacokinetics (GI absorption (**A**), P-glycoprotein substrate (**B**), and CYP3A4 inhibitor (**C**)) of the *Monascus* pigments.

P-glycoprotein is a cell membrane transport protein pumping xenobiotic (including drug molecules) out of cells [40]. This transporter can protect cells against potentially toxic substances by promoting biliary and renal elimination. It could also decrease intestinal absorption and bioavailability of drugs through limiting cytosolic accumulation [40]. Thirty-two (32) MPs including six well-known MPs were not P-glycoprotein substrates, suggesting that these MPs were likely to have high intestinal absorption and bioavailability (Figure 2B).

The cytochrome P450 enzymes are major (accounting for 75%) enzymes involved in drug metabolism. They play a key role in drug elimination through metabolic biotransformation [41]. Members of the CYP3A subfamily, especially CYP3A4 and CYP3A5 (having similar substrate specificities) in adults, are considered to be critical enzymes for drug metabolism, synergistically processing drug molecules with P-glycoprotein to improve the protection of tissues and organisms [42]. Eighteen (18) MPs exhibited in silico inhibition of CYP3A4 (9 yellow, 8 red, and 1 orange) (Figure 2C, Supplementary File 1). Due to the lower clearance and accumulation of the drug or its metabolites,

inhibition of these MPs might cause pharmacokinetics-related drug–drug interactions leading to toxic or other unwanted adverse effects.

3.3. Drug-Likeness and Bioavailability

The drug-likeness of 61 MPs were also predicted using SwissADME building on the Lipinski's rule-of-five [34]. There were 55 MPs having no violation and 6 MPs (1 yellow and 5 red) having one violation of rule-of-five. The one yellow MP (i.e., Y3), had 6 (instead of ≤ 5) hydrogen bond donors; and five red MPs (i.e., N-glucosylrubropunctamine, N-glucosylmonascorubramine, N-glutarylmonascorubramine, Isolate MPs 1, and Isolate MPs 2), had mol. wt. greater than 500. (See Supplementary File 1).

The Bioavailability Score is a semi-quantitative rule-based score relying on total charge, TPSA, and violation to the Lipinski filter, with four classes of probabilities (11%, 17%, 56% or 85%) that compounds have >10% bioavailability in rat or measurable Caco-2 permeability [37]. A score of 55% means the compound passes the rule-of-five, and a score of 17% is a fail [37]. The bioavailability score results showed that most of the MPs have moderate bioavailability (0.55–0.56), while only one yellow MPs has low bioavailability (0.11) (Figure 3).
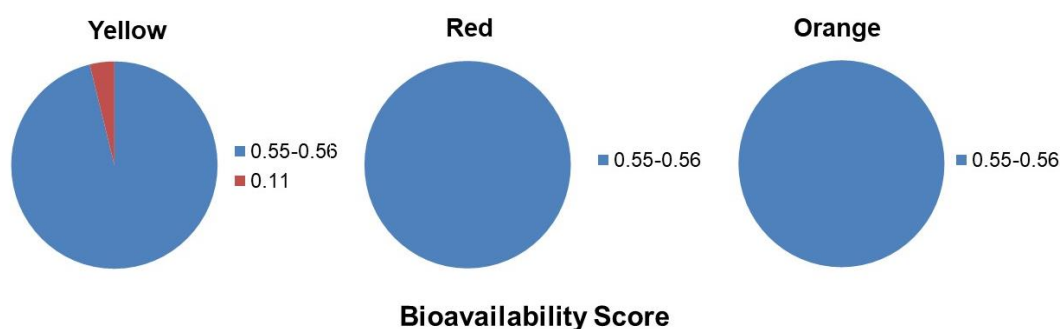

Figure 3. Distribution of drug-likeness (Lipinski range and Bioavailability scores) of the *Monascus* pigments.

The Bioavailability radar of 6 well-known MPs was shown in Figure 4. All six main *Monascus* pigments had physicochemical profiles that makes them suitable for oral administration. Moreover, the six known MPs had bioavailability values that were inside the desired range for enhanced bioavailability.

3.4. Molecular Docking of HMGR and Lipase with Monascus Pigments

3.4.1. HMGR Receptor

The best molecular docking poses of the six main *Monascus* pigments and monacolin K (see structures in Figure 5) interactions with the active site of HMGR are shown in Table 2 and Figure 6. The results indicate affinity energies (kJ/mol) and dissociation constants (Ki) for monascin, ankaflavin, rubropunctatin, monascorubrin, rubropunctamine, monascorubramine, monankarin A, monankarin B and monacolin K (Table 2). The findings suggest that, compared to monacolin K, six main MPs had lower inhibitory properties of HMGR. These results agree with a previous in vitro study by Jeun, et al. [43] who reported that the red and orange pigments exhibited lower inhibitory levels (36%, 15%) against HMGR compared with monacolin K (98%). On the other hand, in their in vitro experiments, the total cholesterol (TC) level of mouse serum was reduced 16% by orange pigments and 9% by monacolin K [43]; but the mechanism of in vitro regulation is not well-known, and therefore warrants further study.
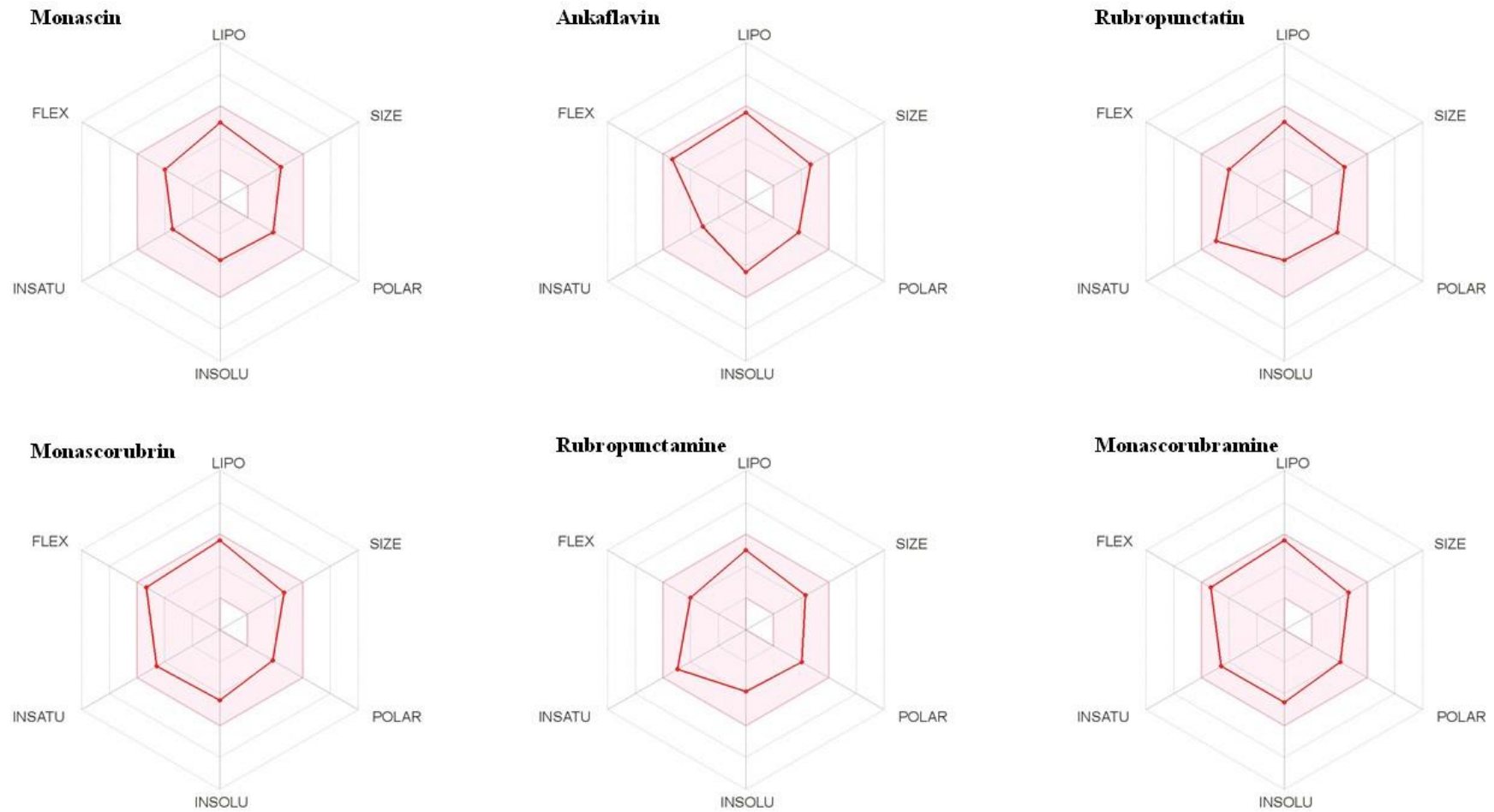
Figure 4. Bioavailability radar of the *Monascus* pigments based on physicochemical indices ideal for oral bioavailability. LIPO, Lipophilicity: $-0.7 < \text{XLOGP3} < þ5$; SIZE, Molecular size: 150 g/mol < mol. wt. < 500 g/mol; POLAR, Polarity: 20 Å2 < TPSA <130 Å2; INSOLU, Insolubility: 0 < Log S (ESOL) < 6; INSATU, Insaturation: 0.25 < Fraction Csp3 < 1; FLEX, Flexibility: 0 < Number of rotatable bonds < 9. The coloured zone is the suitable physicochemical space for oral bioavailability.

Monascin

Ankaflavin

Rubropunctatin

Monascorubrin

Rubropunctamine

Monascorubramine

Monacolin K
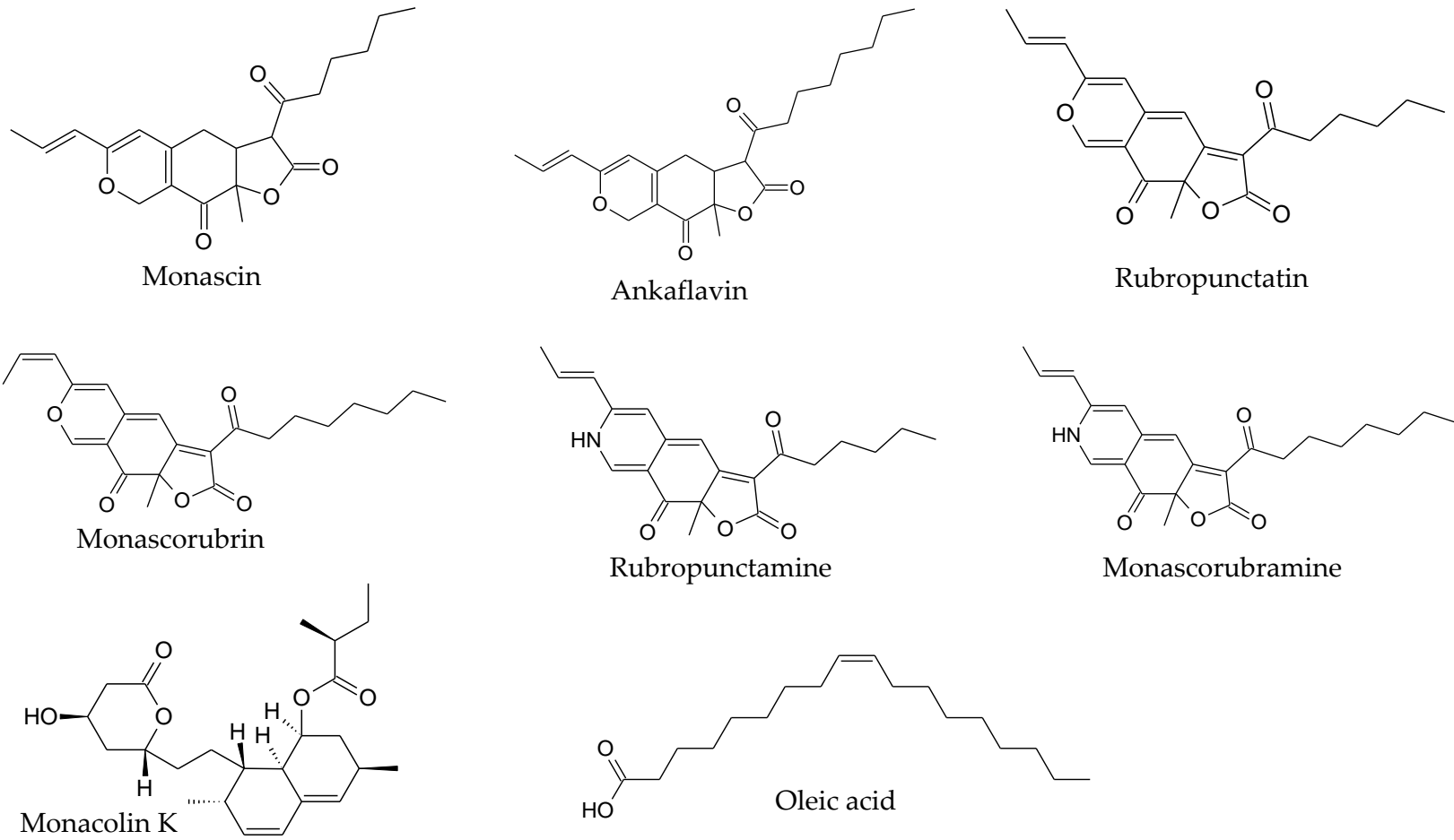
Oleic acid

Figure 5. Structures of six main *Monascus* pigments, monacolin K, and oleic acid.

Table 2. Predicted binding energies and computational dissociation constant of *Monascus* pigments with HMG-CoA reductase (HMGR) (PDB: 1HW9).

Ligand	Affinity Energy (kJ/mol)	K_i (µM)
Monascin	−28.88	8.66
Ankaflavin	−28.88	8.66
Rubropunctatin	−28.89	8.63
Monascorubrin	−28.89	8.63
Rubropunctamine	−28.05	12.11
Monascorubramine	−26.79	20.14
Monacolin K	−30.98	3.71
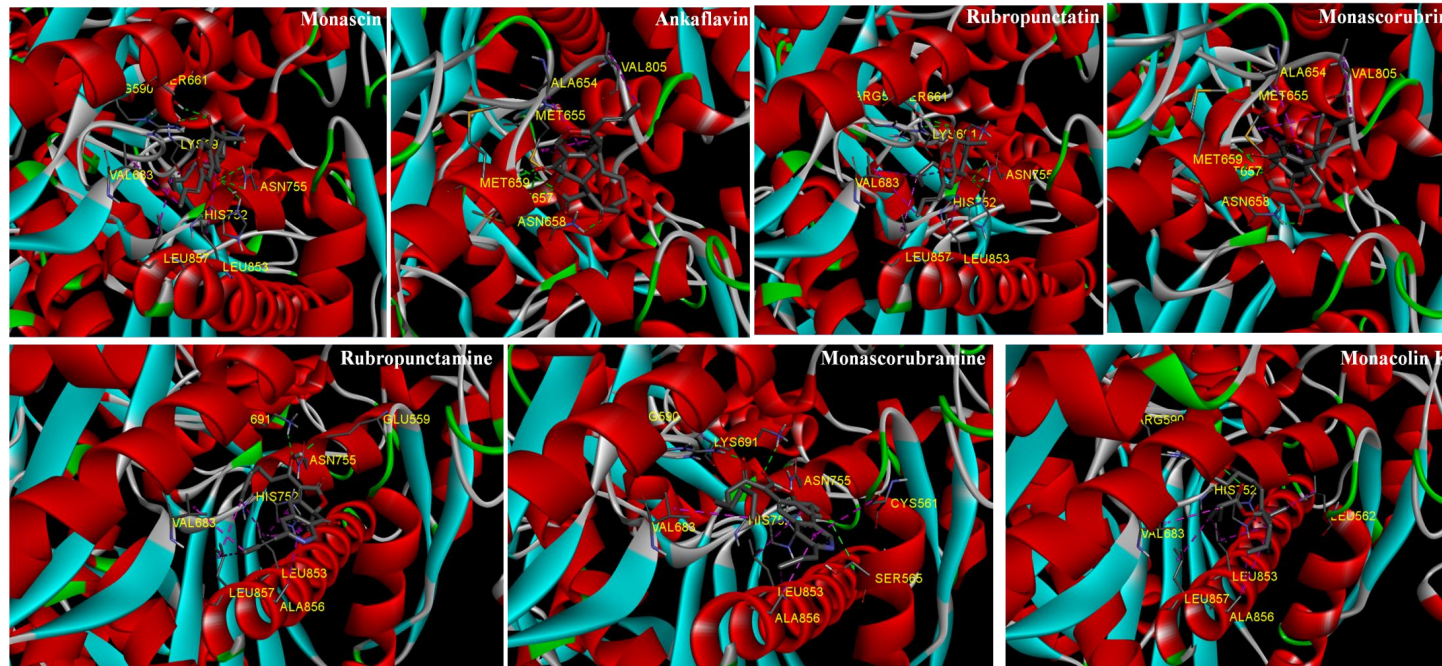
Figure 6. Predicted binding mode of *Monascus* pigments to HMGR (PDB: 1HW9). The best scored docking pose is shown. Green dashed lines are hydrogen bonds, and purple dashed lines are hydrophobic interactions.

In previous docking studies of statins and other chemicals with HMGR, the dissociation constants (K_i) are usually underestimated compared with the in vitro experimental data [44,45]. Therefore, the estimated affinity energies and dissociation constants (K_i) could only be useful at a qualitative level.

The best poses of each MPs and monacolin K were stabilized by hydrophobic interactions and hydrogen bonds with simvastatin binding pockets of HMGR (Figure 6). Four MPs (monascin, rubropunctatin, rubropunctamine and monascorubramin) and monacolin K mainly occupied a hydrophobic pocket with polar groups via hydrogen bonds and hydrophobic interactions with Arg590, Asn755, His752, Leu853, Leu857, Lys691, and Val683. These interactions are similar to a previous study of docking statins and simvastatin to HMGR [45]. However, two other MPs, ankaflavin and monascorubrin mainly occupied simvastatin binding pockets of HMGR via different residues, including Ala654, Asn658, Met655, Met657, Met659, Ser661, and Val805 (Table 3). Those residues could be a new hydrophobic region that needs experimental validation.

Table 3. HMGR (PDB: 1HW9) interact with docked MPs. (●: hydrophobic interactions; ▲: hydrogen bonds).

	Monascin	Ankaflavin	Rubropunctatin	Monascorubrin	Rubropunctamine	Monascorubramine	Monacolin K
GLU559					▲		
CYS561						●	
LEU562							●
SER565						▲	
ARG590	▲		▲			▲	▲
ALA654		●		●			
MET655		●		●			
MET657		▲		▲			
ASN658		▲		▲			
MET659		▲		▲			
SER661	▲		▲				
VAL683	●		●		●	●	●
LYS691	▲		▲		▲	▲	
LYS735							
HIS752	▲		▲		●	▲	●
ASN755	▲		▲		▲	▲	
VAL805		●		●			
GLY806							
GLY807							
GLY808							
LEU853	●		●		●	●	●
ALA856					●	●	●
LEU857	●		●		●		●

The interacting residues, number and distance of hydrogen bonds in the docking model of the six main MPs and Monacolin K within HMGR have been shown in Table 4. The functional importance of hydrogen bonds contributing to inhibition of enzyme activity in the docking experiment has been reported in many previous studies [33,46,47]. However, Monacolin K with only two hydrogen bonds showed higher inhibitory properties compared with MPs with more hydrogen bonds (3–6), suggesting hydrophobic interactions could be more important when docking to simvastatin binding pockets of HMGR. This result is in good agreement with the conclusions drawn by Ressaissi, et al. [45].

3.4.2. Lipase Receptor

The best molecular docking poses of the six main MPs and oleic acid within the active site of lipase is shown in Table 5 and Figure 7. Figure 5 shows the structures of oleic acid. Table 5 shows affinity energies and dissociation constants (K_i) of monascin, ankaflavin, rubropunctatin, monascorubrin, rubropunctamine, monascorubramine and oleic acid. The results suggest that compared to oleic acid, six MPs have higher lipase-inhibitory activities, and monascorubrin and rubropunctamine had the best binding affinity for lipase of all the MPs. These findings agree with previous research that three MPs (monascin, monasuore B, and ankaavin) exerted lipase-inhibitory effects [20].

Table 4. Hydrogen bonds observed in the best scored docking model of the six main MPs and Monacolin K within HMGR (PDB: 1HW9).

HMGR Residues in H-Bonding	Number of H-Bonds and Their Corresponding Distance (Å)						
	Monascin	Ankaflavin	Rubropunctatin	Monascorubrin	Rubropunctamine	Monascorubramine	Monacolin K
GLU559:OE2					1(1.98)		
ARG590:HH11							1(2.03)
ARG590:HH21						1(1.83)	1(3.01)
ARG590:HH22	1(2.31)		1(2.40)				
MET657:HN		1(2.77)		1(2.73)			
MET659:HN		1(2.23)		1(2.41)			
ASN658:HD21		1(2.03)		1(2.14)			
ASN658:HN		2(2.16, 2.23)		2(2.38, 2.16)			
SER661:HG	1(2.34)		1(2.58)				
LYS691:HZ3	1(2.40)		1(2.31)		1(2.62)	1(2.40)	
HIS752:HD1	1(2.75)		1(2.50)			1(2.60)	
ASN755:HD21	1(2.82)		1(2.68)			1(2.53)	
ASN755:HD22	1(2.71)		1(2.84)		1(2.21)		
Total	6	5	6	5	3	4	2

Table 5. Predicted binding energies and computational dissociation constant of *Monascus* pigments with lipase (PDB: 1EHT).

Ligand	Affinity Energy (kJ/mol)	K_i (µM)
Monascin	−28.03	12.19
Ankaflavin	−28.87	8.70
Rubropunctatin	−25.52	33.59
Monascorubrin	−29.29	7.35
Rubropunctamine	−29.29	7.35
Monascorubramine	−24.69	47.08
Oleic acid	−19.66	357.23

Lipase inhibitors have been used as commercial anti-obesity drugs through their ability to prevent or control the hydrolysis of dietary fats into absorbable glycerol and free fatty acids [48]. In a previous in vivo studies, the weights of rats were reduced significantly by two yellow MPs, monascin and ankaflavin [49], but the weights of mice were not significantly changed by red and orange MPs [43]. The anti-obesity effects of *Monascus* pigment derivatives have also been reported in mice, and it is assumed that this anti-obesity effects were caused by inhibition of lipases [48]. In fact, Liu, et al. [50] and Chen, et al. [51] reported that an extract of *Monascus* fermented rice, Ankascin 568 (containing monascin and ankaflavin), significantly reduced the levels of serum total cholesterol and low-density lipoprotein cholesterol in human clinical studies. However, to date, the in vitro inhibitory effects on pure lipase by the six main MPs in this study have never been reported in the published literature. The outcomes of this study show that these six MPs have the potential to act as inhibitors of lipase.

The best poses of each MPs and oleic acid were mainly stabilized by hydrogen bonds, and hydrophobic interactions (Figure 7). In the previous study of Fang, et al. [20], the interactions of MPs with lipase were assumed to be located between two loops: the lid-domain loop (residues 237 to 261) and the β5 loop (residues 75 to 84), and these indirectly affected the active site. However, in this study, there were only a few interacting residues of MPs-lipase located in the two loops (only Ile249) (Table 6). Three MPs (monascin, ankaflavin, monascorubrin,) shared similar interacting residues via hydrogen bonds, as well as hydrophobic and electrostatic interactions with Asn89, Asp 273, Asn272, Lys269, Phe336 (Table 6). Rubropunctamine had only two interacting residues (Lys269, Phe336), but had the highest binding affinity of the six MPs; whereas for monascorubramine, although it also had only two interacting residues (Ile249, Lys269), it showed the lowest binding affinity. This implies that Phe336 could play an important role in stabilizing MPs-lipase interactions.
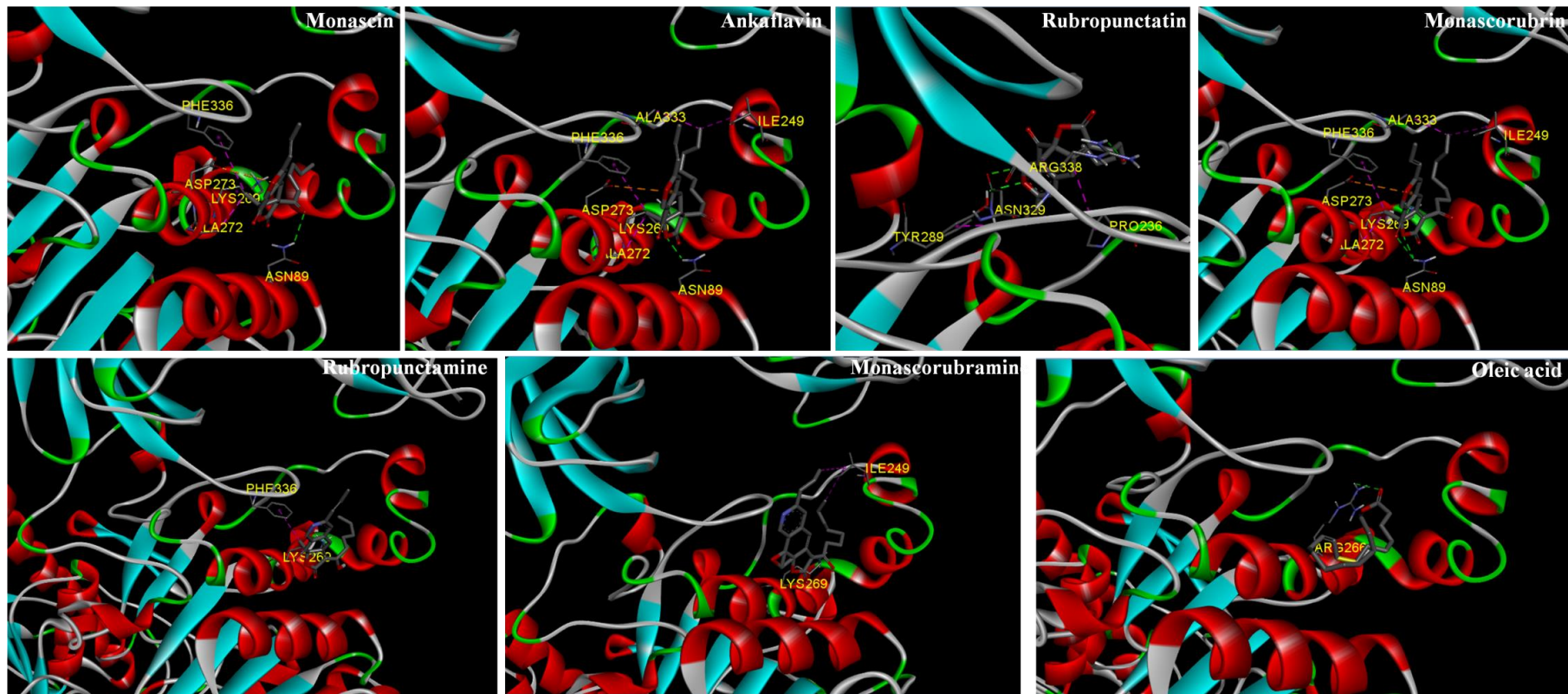
Figure 7. Predicted binding mode of *Monascus* pigments to lipase (PDB: 1EHT). The best scored docking pose is shown. Green dashed lines are hydrogen bonds, purple dashed lines are hydrophobic interactions, and orange dashed lines are electrostatic bonds.

Table 6. Lipase (PDB: 1EHT) interacts with docked *Monascus* pigments. (•: hydrophobic interactions; ▲: hydrogen bonds; ■: electrostatic bonds).

	Monascin	Ankaflavin	Rubropunctatin	Monascorubrin	Rubropunctamine	Monascorubramine	Oleic Acid
ASN89	▲	▲		▲			
PRO236			•				
ILE249		•		•		•	
LYS269	•	•		•	•	▲	
ARG266							▲
ALA272	•	•		•			
ASP273	■	■		■			
TYR289			•▲				
ASN329			▲				
ALA333		•		•			
PHE336	•	•		•	•		
ARG338			•▲				

The interacting residues of hydrogen bonds of the six MPs and oleic acid within lipase are shown in Table 7. Oleic acid interacted with one hydrogen bond and showed lowest inhibitory property. Rubropunctamine however, did not have any hydrogen bond interaction and yet showed the highest inhibitory properties. This seems to suggest that hydrogen bonds are not important in lipase docking.

Table 7. Hydrogen bonds observed in the best scored docking model of the six main MPs and Oleic acid within lipase (PDB: 1EHT).

Lipase Residues in H-Bonding	Number of H-Bonds and Their Corresponding Distance (Å)						
	Monascin	Ankaflavin	Rubropunctatin	Monascorubrin	Rubropunctamine	Monascorubramine	Oleic Acid
ASN89:HD21	1(2.92)						
ASN89:HD22		1(2.32)		2(2.43, 3.05)			
ARG266:HH21							1(2.72)
LYS269:CA						1(3.43)	
TYR289:HH			1(2.54)				
ASN329:OD1			1(3.30)				
ARG338:HH11			1(2.77)				
Total	1	1	3	2	0	1	1

4. Conclusions

In this study, in silico evaluation of physicochemical properties, pharmacokinetics, and drug-likeness of 61 *Monascus* pigments (MPs) was done using the SwissADME tool. Physicochemical features of MPs showed desirable lipophilic drug-likeness, including molecular weight (236 to 543), TPSA (44.76 to 179.77), lipophilicity (−0.81 to 4.14), and water solubility (−4.94 to −0.77.). Most (55) of the MPs met all conditions of Lipinski's rule-of-five of the filter (6 MPs had one violation each).

Pharmacokinetics (gastrointestinal absorption, interaction with P-glycoprotein, inhibition of CYP3A4) and bioavailability predictions showed that most of the MPs had high absorption and bioavailability. However, 18 MPs were predicted to be inhibitors of cytochrome P450 3A4 (CYP3A4), one of the key oxidizing enzymes responsible for clearing xenobiotics from the body. An interference with the activity of CYP3A4 means these MPs may cause pharmacokinetics-related drug–drug interactions that may lead to adverse effects when taken together with other drugs. Among these 18 MPs were 8 red (mostly rubropunctamine, monascorubramine, and Monascopyridine derivatives) 1 orange (monapilol A), and 9 yellow (monankarin derivatives, monapurone derivatives, and rubropunctin) pigments (See Supplementary File 1). The evaluation of drug-likeness and bioavailability showed that most MPs have good drug-like properties, are suitable for oral administration, and had moderate bioavailability.

A docking model for HMGR and lipase active sites was developed using an automated docking approach. Compared to monacolin K, six main MPs had lower inhibitory properties of HMGR, and ankaflavin and monascorubrin had unique binding residues, perhaps showing binding at a new

hydrophobic region. The results of lipase docking suggested that, compared to oleic acid, six MPs have higher lipase-inhibitory activities, and we found the hydrophobic Phe336 could play an important role in stabilizing MPs-lipase interactions. Although hydrogen bonds are usually important for interactions between ligand and proteins, in this study, they were not found to be important for docking of lipases.

The limitation of this study is that there are many factors involved in metabolism of lipids and control of hyperlipidemia, and that HMG-CoA reductase and pancreatic lipase [18,20] are not the only targets. It is understandable that MPs may also have inhibiting or activating effects on other proteins involved in lipid metabolism. In vitro and in vivo studies involving interactions of MPs and these other protein targets should therefore be studied to gain a complete picture of the effects of MPs on hyperlipidemia.

Moreover, in silico data are usually underestimated or overestimated when compared with in vitro and in vivo experimental data. This suggests that in silico findings need experimental validation from in vitro and in vivo studies to confirm the hypolipidemic effects of MPs. Another important recommendation is the need to for in vivo research to be done on the effects of individual MPs on the activities of HMG-CoA reductase and pancreatic lipase, thus helping to unravel how these MPs control hyperlipidemia.

Supplementary Materials: The following are available online at http://www.mdpi.com/2311-5637/6/4/111/s1.

Author Contributions: Conceptualization, D.J.; methodology, D.J.; software, N.S. and D.J.; validation, N.S., D.A. and D.J.; formal analysis, N.S. and D.J.; investigation, N.S. and D.J.; data curation, N.S.; writing—original draft preparation, N.S. and D.J.; writing—review and editing, N.S., D.A. and D.J.; supervision, D.A. All authors have read and agreed to the published version of the manuscript.

Conflicts of Interest: The authors declare no conflict of interest.

References

1. Zhang, Y.; Wang, Z.; Jin, G.; Yang, X.; Zhou, H. Regulating dyslipidemia effect of polysaccharides from Pleurotus ostreatus on fat-emulsion-induced hyperlipidemia rats. *Int. J. Biol. Macromol.* **2017**, *101*, 107–116. [CrossRef] [PubMed]
2. Liang, J.-X.; Zhang, Q.-Q.; Huang, Y.-F.; Pang, H.-Q.; Liu, X.-G.; Gao, W.; Li, P.; Yang, H. Comprehensive chemical profiling of monascus-fermented rice product and screening of lipid-lowering compounds other than monacolins. *J. Ethnopharmacol.* **2019**, *238*, 111879. [CrossRef] [PubMed]
3. Harikumar, K.; Althaf, S.A.; Kumar, B.K.; Ramunaik, M.; Suvarna, C.H. A review on hyperlipidemic. *Int. J. Nov. Trends Pharm. Sci.* **2013**, *3*, 59–71.
4. Liu, J.; Zhang, J.; Shi, Y.; Grimsgaard, S.; Alraek, T.; Fønnebø, V. Chinese red yeast rice (Monascus purpureus) for primary hyperlipidemia: A meta-analysis of randomized controlled trials. *Chin. Med.* **2006**, *1*, 4. [CrossRef] [PubMed]
5. Tanner, R.M.; Colantonio, L.D.; Kilgore, M.L.; Mefford, M.T.; Chachappan, D.T.; Mues, K.E.; Safford, M.M.; Rosenson, R.S.; Muntner, P. Low-density lipoprotein cholesterol levels among individuals experiencing statin-associated symptoms: Data from the REasons for Geographic And Racial Differences in Stroke (REGARDS) study. *J. Clin. Lipidol.* **2020**, *14*, 720–729. [CrossRef]
6. Bellosta, S. Safety of Statins: Focus on Clinical Pharmacokinetics and Drug Interactions. *Circulation* **2004**, *109*, III50–III57. [CrossRef]
7. McGinnis, B.; Olson, K.L.; Magid, D.; Bayliss, E.; Korner, E.J.; Brand, D.W.; Steiner, J.F. Dyslipidemia: Factors related to adherence to statin therapy. *Ann. Pharmacother.* **2007**, *41*, 1805–1811. [CrossRef]
8. Butalia, S.; Lee-Krueger, R.C.; McBrien, K.A.; Leung, A.A.; Anderson, T.J.; Quan, H.; Naugler, C.; Chen, G.; Campbell, D.J. Barriers and Facilitators to Using Statins: A Qualitative Study With Patients and Family Physicians. *CJC Open* **2020**, in press. [CrossRef]
9. Berent, T.; Berent, R.; Steiner, S.; Sinzinger, H. Statin-induced muscular side effects at rest and exercise—An anatomical mapping. *Atheroscler. Suppl.* **2019**, *40*, 73–78. [CrossRef]
10. Rojas-Fernandez, C.; Hudani, Z.; Bittner, V. Statins and Cognitive Side Effects. *Endocrinol. Metab. Clin. North Am.* **2016**, *45*, 101–116. [CrossRef]

11. Thompson, P.D.; Panza, G.; Zaleski, A.; Taylor, B. Statin-Associated Side Effects. *J. Am. Coll. Cardiol.* **2016**, *67*, 2395–2410. [CrossRef] [PubMed]

12. Gonnelli, S.; Caffarelli, C.; Stolakis, K.; Cuda, C.; Giordano, N.; Nuti, R. Efficacy and Tolerability of a Nutraceutical Combination (Red Yeast Rice, Policosanols, and Berberine) in Patients with Low-Moderate Risk Hypercholesterolemia: A Double-Blind, Placebo-Controlled Study. *Curr. Ther. Res.* **2015**, *77*, 1–6. [CrossRef] [PubMed]

13. Wang, T.; Lin, T. Monascus Rice Products. *Adv. Food Nutr. Res.* **2007**, *53*, 123–159. [CrossRef] [PubMed]

14. Li, C.; Zhu, Y.; Wang, Y.; Zhu, J.-S.; Chang, J.; Kritchevsky, D. Monascus purpureus-fermented rice (red yeast rice): A natural food product that lowers blood cholesterol in animal models of hypercholesterolemia. *Nutr. Res.* **1998**, *18*, 71–81. [CrossRef]

15. Lin, Y.-L.; Wang, T.-H.; Lee, M.-H.; Su, N.-W. Biologically active components and nutraceuticals in the Monascus-fermented rice: A review. *Appl. Microbiol. Biotechnol.* **2008**, *77*, 965–973. [CrossRef] [PubMed]

16. Becker, D.J.; Gordon, R.Y.; Halbert, S.C.; French, B.; Morris, P.B.; Rader, D.J. Red Yeast Rice for Dyslipidemia in Statin-Intolerant Patients. *Ann. Intern. Med.* **2009**, *150*, 830–839. [CrossRef] [PubMed]

17. Borden, W.B. Red yeast rice for dyslipidemia in statin-intolerant patients. *Curr. Atheroscler. Rep.* **2010**, *12*, 11–13. [CrossRef] [PubMed]

18. Lee, C.-L.; Tsai, T.-Y.; Wang, J.-J.; Pan, T.-M. In vivo hypolipidemic effects and safety of low dosage Monascus powder in a hamster model of hyperlipidemia. *Appl. Microbiol. Biotechnol.* **2005**, *70*, 533–540. [CrossRef]

19. Zhou, W.; Guo, R.; Guo, W.; Hong, J.; Li, L.; Ni, L.; Sun, J.; Liu, B.; Rao, P.; Lv, X.-C. Monascus yellow, red and orange pigments from red yeast rice ameliorate lipid metabolic disorders and gut microbiota dysbiosis in Wistar rats fed on a high-fat diet. *Food Funct.* **2019**, *10*, 1073–1084. [CrossRef]

20. Fang, Y.-X.; Song, H.-P.; Liang, J.-X.; Li, P.; Yang, H. Rapid screening of pancreatic lipase inhibitors from Monascus-fermented rice by ultrafiltration liquid chromatography-mass spectrometry. *Anal. Methods* **2017**, *9*, 3422–3429. [CrossRef]

21. Agboyibor, C.; Kong, W.-B.; Chen, D.; Zhang, A.-M.; Niu, S.-Q. Monascus pigments production, composition, bioactivity and its application: A review. *Biocatal. Agric. Biotechnol.* **2018**, *16*, 433–447. [CrossRef]

22. Yuliana, A.; Singgih, M.; Julianti, E.; Blanc, P.J. Derivates of azaphilone Monascus pigments. *Biocatal. Agric. Biotechnol.* **2017**, *9*, 183–194. [CrossRef]

23. Gao, J.-M.; Yang, S.-X.; Qin, J.-C. Azaphilones: Chemistry and Biology. *Chem. Rev.* **2013**, *113*, 4755–4811. [CrossRef] [PubMed]

24. Feng, Y.; Shao, Y.; Chen, F. Monascus pigments. *Appl. Microbiol. Biotechnol.* **2012**, *96*, 1421–1440. [CrossRef]

25. Blanc, P.J. Characterization of monascidin A from Monascus as citrinin. *Int. J. Food Microbiol.* **1995**, *27*, 201–213. [CrossRef]

26. Wang, Y.; Gao, H.; Xie, J.; Li, X.; Huang, Z. Effects of some flavonoids on the mycotoxin citrinin reduction by Monascus aurantiacus Li AS3.4384 during liquid-state fermentation. *AMB Express* **2020**, *10*, 1–10. [CrossRef]

27. Liang, B.; Du, X.-J.; Li, P.; Sun, C.-C.; Wang, S. Investigation of Citrinin and Pigment Biosynthesis Mechanisms in Monascus purpureus by Transcriptomic Analysis. *Front. Microbiol.* **2018**, *9*, 1374. [CrossRef]

28. Liu, L.; Zhao, J.; Huang, Y.; Xin, Q.; Wang, Z. Diversifying of Chemical Structure of Native Monascus Pigments. *Front. Microbiol.* **2018**, *9*, 3143. [CrossRef]

29. Saleh-E-In, M.; Roy, A.; Al-Mansur, M.A.; Hasan, C.M.; Rahim, M.; Sultana, N.; Ahmed, S.; Islam, R.; Amoo, S.O. Isolation and in silico prediction of potential drug-like compounds from Anethum sowa L. root extracts targeted towards cancer therapy. *Comput. Biol. Chem.* **2019**, *78*, 242–259. [CrossRef]

30. Yi, F.; Li, L.; Xu, L.-J.; Meng, H.; Dong, Y.-M.; Liu, H.-B.; Xiao, P.-G. In silico approach in reveal traditional medicine plants pharmacological material basis. *Chin. Med.* **2018**, *13*, 33. [CrossRef]

31. Agyei, D.; Bambarandage, E.; Udenigwe, C.C. The Role of Bioinformatics in the Discovery of Bioactive Peptides. *Encycl. Food Chem.* **2019**, 337–344. [CrossRef]

32. Ji, D.; Udenigwe, C.C.; Agyei, D. Antioxidant peptides encrypted in flaxseed proteome: An in silico assessment. *Food Sci. Hum. Wellness* **2019**, *8*, 306–314. [CrossRef]

33. Ji, D.; Xu, M.; Udenigwe, C.C.; Agyei, D. Physicochemical characterisation, molecular docking, and drug-likeness evaluation of hypotensive peptides encrypted in flaxseed proteome. *Curr. Res. Food Sci.* **2020**, *3*, 41–50. [CrossRef] [PubMed]

34. Lipinski, C.A.; Lombardo, F.; Dominy, B.W.; Feeney, P.J. Experimental and computational approaches to estimate solubility and permeability in drug discovery and development settings. *Adv. Drug Deliv. Rev.* **1997**, *23*, 3–25. [CrossRef]

35. Daina, A.; Zoete, V. A BOILED-Egg To Predict Gastrointestinal Absorption and Brain Penetration of Small Molecules. *ChemMedChem* **2016**, *11*, 1117–1121. [CrossRef]

36. Isyaku, Y.; Uzairu, A.; Uba, S. Computational studies of a series of 2-substituted phenyl-2-oxo-, 2-hydroxyl- and 2-acylloxyethylsulfonamides as potent anti-fungal agents. *Heliyon* **2020**, *6*, e03724. [CrossRef]

37. Daina, A.; Michielin, O.; Zoete, V. SwissADME: A free web tool to evaluate pharmacokinetics, drug-likeness and medicinal chemistry friendliness of small molecules. *Sci. Rep.* **2017**, *7*, 42717. [CrossRef]

38. Mokhnache, K.; Madoui, S.; Khither, H.; Charef, N. Drug-likeness and pharmacokinetics of a bis-phenolic ligand: Evaluations by computational methods. *Sch. J. App. Med. Sci.* **2019**, *1*, 167–173.

39. Delaney, J.S. ESOL: Estimating Aqueous Solubility Directly from Molecular Structure. *J. Chem. Inf. Comput. Sci.* **2004**, *44*, 1000–1005. [CrossRef]

40. Wolking, S.; Schaeffeler, E.; Lerche, H.; Schwab, M.; Nies, A.T. Impact of Genetic Polymorphisms of ABCB1 (MDR1, P-Glycoprotein) on Drug Disposition and Potential Clinical Implications: Update of the Literature. *Clin. Pharmacokinet.* **2015**, *54*, 709–735. [CrossRef]

41. Guengerich, F.P. Cytochrome P450 and Chemical Toxicology. *Chem. Res. Toxicol.* **2008**, *21*, 70–83. [CrossRef] [PubMed]

42. Van Waterschoot, R.A.B.; Schinkel, A.H. A Critical Analysis of the Interplay between Cytochrome P450 3A and P-Glycoprotein: Recent Insights from Knockout and Transgenic Mice. *Pharmacol. Rev.* **2011**, *63*, 390–410. [CrossRef]

43. Jeun, J.; Jung, H.; Kim, J.H.; Kim, Y.O.; Youn, S.H.; Shin, C.S. Effect of the monascus pigment threonine derivative on regulation of the cholesterol level in mice. *Food Chem.* **2008**, *107*, 1078–1085. [CrossRef]

44. Medina-Franco, J.L.; López-Vallejo, F.; Rodríguez-Morales, S.; Castillo, R.; Chamorro, G.; Tamariz, J. Molecular docking of the highly hypolipidemic agent α-asarone with the catalytic portion of hmg-coa reductase. *Bioorganic Med. Chem. Lett.* **2005**, *15*, 989–994. [CrossRef] [PubMed]

45. Ressaissi, A.; Attia, N.; Falé, P.L.; Pacheco, R.; Victor, B.L.; Machuqueiro, M.; Serralheiro, M.L. Isorhamnetin derivatives and piscidic acid for hypercholesterolemia: Cholesterol permeability, HMG-CoA reductase inhibition, and docking studies. *Arch. Pharmacal Res.* **2017**, *40*, 1278–1286. [CrossRef] [PubMed]

46. He, R.; Aluko, R.E.; Ju, X.-R. Evaluating Molecular Mechanism of Hypotensive Peptides Interactions with Renin and Angiotensin Converting Enzyme. *PLoS ONE* **2014**, *9*, e91051. [CrossRef]

47. Jimsheena, V.; Gowda, L.R. Arachin derived peptides as selective angiotensin I-converting enzyme (ACE) inhibitors: Structure–activity relationship. *Peptides* **2010**, *31*, 1165–1176. [CrossRef]

48. Kim, J.-H.; Kim, Y.O.; Jeun, J.; Choi, D.-Y.; Shin, C.S. L-Trp andL-Leu-OEt Derivatives of the Monascus Pigment Exert High Anti-Obesity Effects on Mice. *Biosci. Biotechnol. Biochem.* **2010**, *74*, 304–308. [CrossRef]

49. Lee, C.-L.; Wen, J.-Y.; Hsu, Y.-W.; Pan, T.-M. Monascus-Fermented Yellow Pigments Monascin and Ankaflavin Showed Antiobesity Effect via the Suppression of Differentiation and Lipogenesis in Obese Rats Fed a High-Fat Diet. *J. Agric. Food Chem.* **2013**, *61*, 1493–1500. [CrossRef]

50. Liu, S.-F.; Wang, Y.-R.; Shen, Y.-C.; Chen, C.-L.; Huang, C.-N.; Pan, T.-M.; Wang, C.-K. A randomized, double-blind clinical study of the effects of Ankascin 568 plus on blood lipid regulation. *J. Food Drug Anal.* **2018**, *26*, 393–400. [CrossRef]

51. Chen, C.-L.; Tseng, J.-H.; Hsiao, S.-H.; Pan, T.-M. A Randomized, Double-Blind Clinical Study on Blood Pressure Reduction and Blood Lipid Profile Amelioration on Treatment with Ankascin 568. *Chin. J. Physiol.* **2017**, *60*, 158–165. [CrossRef] [PubMed]